Proceedings of the IV ISSPMS'01, Jaszowiec 2001

Optimization of Soft Magnetic Properties in Fe–B and Fe–B–Si Amorphous Alloys Obtained by Melt Spinning Method

P. Kwapuliński*, Z. Stokłosa, A. Chrobak, J. Rasek and G. Haneczok

Institute of Physics and Chemistry of Metals, Silesian University
Bankowa 12, 40-007 Katowice, Poland

In the present paper the process of optimization of soft magnetic properties have been studied by applying different experimental techniques (magnetic measurements, electric measurements, X-ray analysis, and high-resolution electron microscopy observations). It has been shown that an increase in magnetic permeability after optimization annealing can be mainly attributed to annealing out of microvoids.

PACS numbers: 75.50–y, 75.75.+a

1. Introduction

It has been shown that magnetic properties of amorphous alloys obtained by melt spinning technique can be optimised by applying a suitable thermal annealing at temperatures close to the crystallization temperature [1–7]. Using this procedure a material with magnetic permeability of the order of 10^5, coercive field 1–3 A/m and electrical resistivity of about $1.5- - 2$ $\mu\Omega$·m (i.e. 2–3 times higher than the typical values of conventional soft magnetic materials, e.g. Fe–Si alloy) can be obtained. The enhancement of soft magnetic properties is usually attributed to three different processes: (i) a formation of a nanocrystalline phase with the grain size much smaller than the exchange ferromagnetic length, (ii) an annealing out of microvoids formed during the production procedure, and also (iii) a significant decrease in the magnetostriction constant. The role and the efficiency of these processes strongly depend on the chemical composition of the examined material.

*corresponding author; e-mail: pkwapuli@us.edu.pl

The main aim of the present paper is to study the optimization processes in the $Fe_{78}B_{22-x}Si_x$ group of amorphous alloys. This kind of examination essentially has two aspects. On the one hand, the systematic variation of Si content in iron-based alloys allows establishing the role of silicon atoms in optimization procedure and on the other hand, from a practical point of view it is important to find conditions of thermal annealing (temperature and time) causing magnetic properties improvements. Obviously, the understanding of optimization procedure in relatively simple alloys should be considered as a starting point for the examination of more complex materials.

2. Samples and experimental procedure

Experiments were carried out on samples of the $Fe_{78}B_{22-x}Si_x$ (x = 0, 8, 9, and 13) amorphous alloys obtained by melt-spinning technique in the form of ribbons (thickness of about 25 μm). In order to study the optimization processes samples in the "as-quenched" state were annealed for one hour at temperatures from the range 300–950 K (denoted as T_a) with the step of 25 K. After the annealing the following physical quantities were measured at room temperature: (i) initial magnetic permeability μ (Maxwell–Wien bridge at a frequency of 1030 Hz and magnetic field $H = 0.5$ A/m), (ii) magnetic after-effect $\Delta\mu/\mu$ (where $\Delta\mu = \mu(t_1) - \mu(t_2)$ is the difference between magnetic permeability determined at time $t_1 = 30$ s and $t_2 = 1800$ s after demagnetization and μ at t_1), (iii) coercive field H_c (permalloy probe) and (iv) electrical resistivity ρ (four-point probe method).

In order to study the crystallization processes X-ray diffraction analysis (Philips diffractometer) and electron microscopy method (JEM-200B and high resolution JEM 3010) have been used. For all examined alloys electrical resistivity $\rho(T)$ curves were measured as a function of temperature with a heating rate of about 0.5 K/min (the so-called "*in situ*" measurements). For determining the Curie temperature of the examined material measurements of magnetic permeability versus temperature (heating rate 10 K/min) have been used.

3. Experimental results

Figure 1 shows initial magnetic permeability (determined at room temperature) plotted versus one-hour annealing temperature T_a. From this figure it can be recognised that for all examined alloys $\mu(T_a)$ passes by a sharp maximum. The temperature T_a corresponding to $\mu(T_a)$ maximum we define as the one-hour optimization annealing temperature — T_{op}. From Fig. 1 the temperature T_{op} can be determined as 600 K, 675 K, and 625 K for $Fe_{78}B_{22}$, $Fe_{78}B_{14}Si_8$, and $Fe_{78}B_9Si_{13}$ alloys, respectively. For the $Fe_{78}B_{13}Si_9$ alloy the optimization temperature was determined as 675 K, so we have obtained the same value as for the $Fe_{78}B_{14}Si_8$

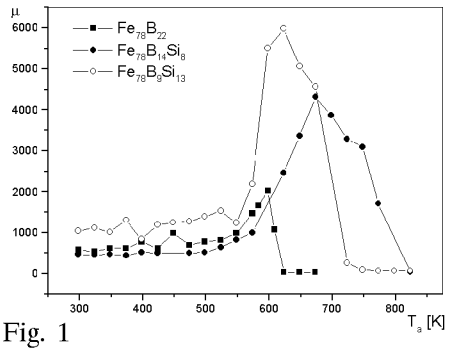

Fig. 1

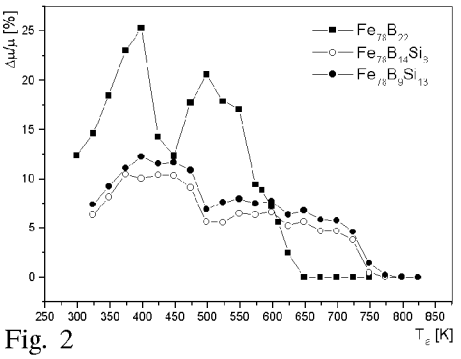

Fig. 2

Fig. 1. Initial magnetic permeability μ measured at room temperature for samples after one-hour annealing at temperature T_{a}.

Fig. 2. Magnetic after-effect $\Delta\mu/\mu$ ($[\mu(t_1) - \mu(t_2)]/\mu(t_1)$, where times $t_1 = 30$ s and $t_2 = 1800$ s after demagnetization), measured at room temperature for samples after one-hour annealing at temperature T_{a}.

alloy. Apparently, the method used for obtaining T_{op} cannot distinguish between these two alloys $Fe_{78}B_{14}Si_8$ and $Fe_{78}B_{13}Si_9$.

Figure 2 presents magnetic after-effect $\Delta\mu/\mu$ plotted versus one-hour annealing temperature T_{a} for different alloys. Such a plot demonstrates the thermal instability of magnetic properties of the examined material. As it was already shown [8–10] magnetic after-effect intensity is directly proportional to the concentration of migrating defects, i.e. in our case to microvoid concentration (free volume). From Fig. 2 it can be recognised that $\Delta\mu/\mu(T_{\mathrm{a}})$ curves exhibit two broad maxima — the first one situated near 400–450 K and the second one at 550–600 K. At higher temperatures ($T_{\mathrm{a}} > \mathrm{T_{op}}$) a drastic decrease in $\Delta\mu/\mu$ value is observed which indicates the annealing out of microvoids.

The results of measurements of coercive field are presented in Fig. 3, where H_{c} is plotted in logarithmic scale versus one-hour annealing temperature T_{a} for

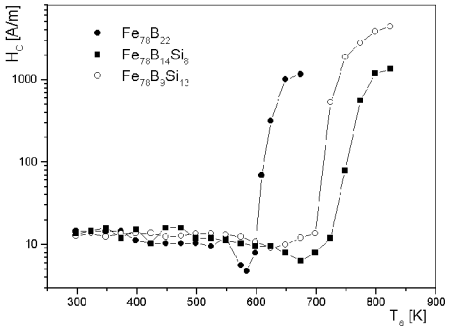

Fig. 3. Coercive force H_{c} measured at room temperature for samples after one-hour annealing at temperature T_{a}.

the $Fe_{78}B_{13}Si_9$ and $Fe_{78}B_{22}$ alloys. The changes of H_c due to annealing procedure up to crystallization are well demonstrated. Comparing the results presented in Figs. 1–3 it can be noticed that the magnetic permeability maximum observed at T_{op} correlates with a minimum of coercive force and also with a decrease in magnetic after-effect intensity. This obviously means that one-hour annealing at temperature T_{op} causes a real improvement of soft magnetic properties.

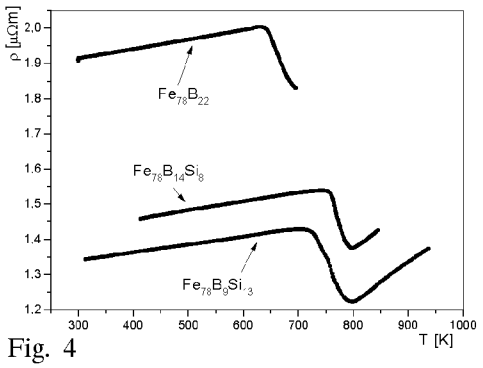

Fig. 4

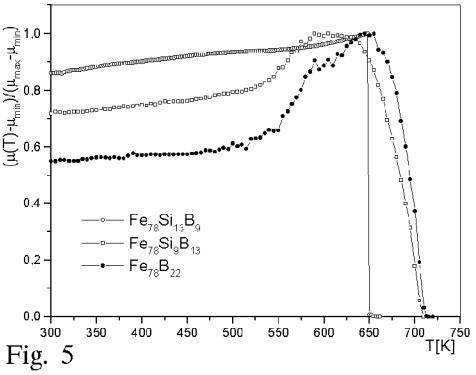

Fig. 5

Fig. 4. Electrical resistivity versus temperature (heating with a rate of 0.5 K/min).
Fig. 5. Normalised magnetic permeability versus temperature (a heating rate of 10 K/min).

The results of "*in situ*" measurements are presented in Figs. 4 and 5, where electrical resistivity curves $\rho(T)$ and normalised magnetic permeability $\mu(T)$ are shown. The drastic decrease in $\rho(T)$ observed at elevated temperatures is due to crystallization phenomena. The characteristic temperature T_1 of the first stage of crystallization process can be determined from the condition $d\rho(T)/dT = 0$. The Curie temperature of the examined alloys is taken as $\mu(T_C) = 0$ (see Fig. 5).

4. Discussion

The characteristic temperatures (i.e. one-hour optimization annealing temperature T_{op}, Curie temperature T_C, and temperature of the first stage of crystallization process T_1) determined from the experimental data presented in preceding section, are plotted versus Si content in Fig. 6. One can notice that in the examined group of amorphous alloys $Fe_{78}B_{22-x}Si_x$ the temperature T_{op} is always lower than T_C. This means obviously that the structural changes responsible for the improvements of soft magnetic properties take place in ferromagnetic phase. For multicomponent alloys (e.g. Fe–X–B_9Si_{13} or Fe–X–Cu_1–B_9Si_{13} (X=Mo, Al, Cr, Zr)), as it was recently shown, the temperature of one-hour optimization annealing can be higher than the Curie temperature [4–6, 11]. Let also notice that according to Fig. 6 the increase in Si content causes a decrease in the Curie tem-

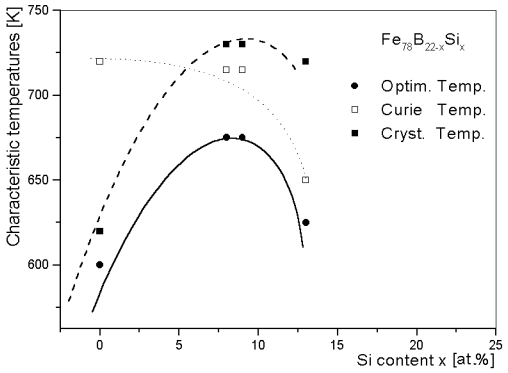

Fig. 6. Characteristic temperatures (i.e. optimization temperature — $T_{\rm op}$, Curie temperature — $T_{\rm C}$, and crystallization temperature — T_1) versus Si content.

perature but in the studied region $T_{\rm op} > {\rm T_C}$. Obviously, a material with relatively high $T_{\rm C}$ is very interesting for practical applications.

The results presented in Fig. 1 show that magnetic permeability μ measured at room temperature for a sample annealed at $T_{\rm a}$ remains nearly constant up to 500 K (550 K). In this temperature range the intensity of magnetic after-effect reflecting thermal instability of the material passes through a distinct maximum (see Fig. 2). This effect is usually attributed to a new rearrangements (a short distance migration) of microvoids formed during fabrication (rapid cooling from liquid phase) [4–6]. As a consequence of it an amorphous alloy at relatively low temperatures tends to a new thermodynamic equilibrium via local microvoid movement. Annealing at higher temperature $T_{\rm a} > 550$ K causes a long-distance microvoid migration, which leads to their annealing out and the intensity of magnetic after-effect rapidly decreases. It is easy to notice that the highest concentration of microvoids was observed for the $Fe_{78}B_{22}$ alloy (see Fig. 2).

As it was already mentioned a strong increase in magnetic permeability observed after annealing at temperature $T_{\rm a} \geq 600$ K (see Fig. 1) can be explained by: (i) a formation of a nanocrystalline structure, (ii) a decrease in the effective magnetostriction constant, and also (iii) an annealing out of microvoids (see Fig. 2). According to the so-called Herzer model with random distribution of anisotropy constant [2, 12–16] the nanocrystallization process should be the most efficient because of $\mu \propto 1/d^6$ (d — the mean grain size). In our case, as it is documented in Figs. 4 and 6 the crystallization process for all studied materials takes place at temperatures higher than $T_{\rm op}$. The difference $T_1 - T_{\rm op}$ according to Fig. 6 increases with Si content, although both temperatures T_1 as well as $T_{\rm op}$ reaches a maximum value for 8–9 at.% of Si (see Fig. 6).

X-ray diffraction analysis and high-resolution electron microscopy (HREM) observations performed for samples annealed at $T_{\rm op}$ show that nanostructural grains in amorphous matrix are observed only for the $Fe_{78}B_{22}$ alloy. This is demon-

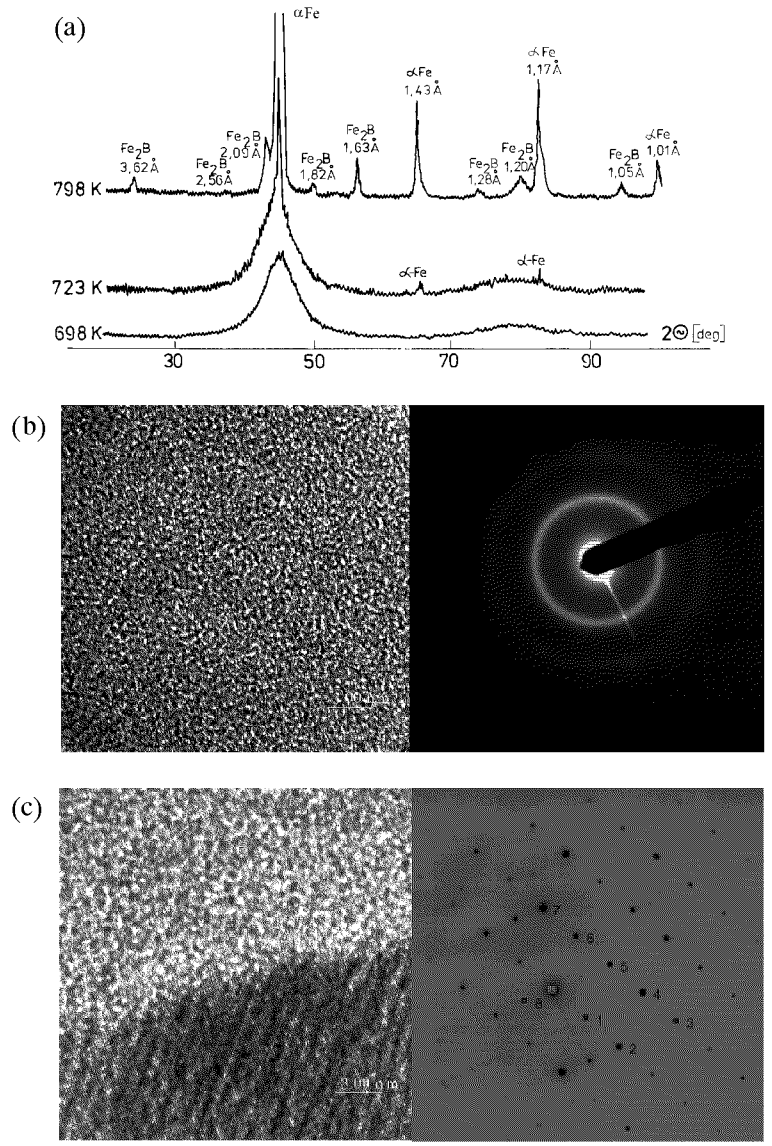

Fig. 7. (a) X-ray diffraction analysis for $Fe_{78}B_9Si_{13}$; (b) HREM image for $Fe_{78}B_9Si_{13}$ annealed at T_{op} (625 K/1 h), (c) HREM image for $Fe_{78}B_{22}$ annealed at T_{op} (450 K/1 h).

strated in Figs. 7a, b, and c, where the analysis of X-ray diffraction for $Fe_{78}B_9Si_{13}$ and HREM images for $Fe_{78}B_9Si_{13}$ and $Fe_{78}B_{22}$ alloys are presented, respectively. In the case of the $Fe_{78}B_{22}$ alloy the difference between T_{op} and T_1 is the smallest and apparently the crystallization during one-hour annealing at T_{op} can occur. Let us notice that the comparison of T_{op} with T_1 has only a limited sense because of different heating procedure used in the experiments. The mean grain size of the

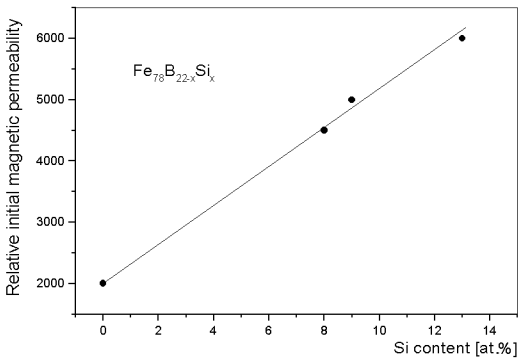

Fig. 8. Initial magnetic permeability determined for samples after optimization annealing plotted versus Si content.

new phase was estimated as 100–150 nm and its volume fraction does not exceed a few percent. For other examined alloys after annealing at T_{op} the nanostructural phase was not detected.

Finally it can be concluded that in the group of examined alloys $Fe_{78}B_{22-x}Si_x$ for $x \neq 0$ the enhancement of soft magnetic properties can be attributed to annealing out of microvoids and nanocrystallization does not play any role. For $x = 0$ (Si free alloy) the discussed improvement of magnetic properties should be attributed to annealing out of microvoids and formation of nanocrystalline phase. The efficiency of the optimization annealing is presented in Fig. 8, where the value of initial magnetic permeability is plotted versus Si content. As it can be recognise μ is directly proportional to Si content.

5. Conclusions

In the present paper the optimization processes of soft magnetic properties in the $Fe_{78}B_{22-x}Si_x$ ($x = 0, 8, 9, 13$) group of amorphous alloys were studied by applying different experimental techniques. The main conclusions can be summarised as follows:

1. Application of one-hour annealing at suitable temperatures causes a strong increase in initial magnetic permeability, which is correlated with a minimum of coercive field and a significant decrease in magnetic after-effect (time/thermal instabilities); the temperature of one-hour optimization annealing depends on Si/B content.
2. The observed increase in magnetic permeability in the $Fe_{78}B_{22-x}Si_x$ alloys with $x = 8, 9, 13$ can be explained by annealing out of microvoids formed during the production process; for the $Fe_{78}B_{22}$ alloy ($x = 0$) annealing out of microvoids should be accompanied by the formation of nanocrystalline phase.

3. Initial magnetic permeability in optimised samples is directly proportional to Si content.

Acknowledgments

This work was partially supported by the State Committee for Scientific Research under grant No. PBZ/KBN-013/T08/47.

References

[1] M.E. McHenry, M.A. Willard, D.E. Laughlin, *Progr. Mater. Sci.* **44,** 291 (1999).

[2] J. Rasek, *Some Diffusion Phenomena in Crystalline and Amorphous Metals*, Silesian University Press, Katowice 2000 (in Polish).

[3] G. Haneczok, J. Rasek, *Def. Diff. Forum* **188-190,** 218 (2001).

[4] P. Kwapuliński, J. Rasek, Z. Stokłosa, G. Haneczok, M. Gigla, *J. Magn. Magn. Mater.* **215-216,** 334 (2000).

[5] Z. Stokłosa, P. Kwapuliński, G. Haneczok, J. Rasek, *J. Phys. (France) IV* **8,** 51 (1998).

[6] P. Kwapuliński, J. Rasek, Z. Stokłosa, G. Haneczok, *J. Magn. Magn. Mater.* **234,** 218 (2001).

[7] H. Matyja, T. Kulik, *Trends in Non Crystalline Solids*, Word Scientific, Singapore 1992, p. 107.

[8] H. Kronmüller, *Philos. Magn. B* **48,** 127 (1983).

[9] B. Zegrodnik, G. Haneczok, J. Rasek, *Mater. Sci. Arch.* **15,** 161 (1994).

[10] T. Egami, *Rapidly Quenched Metals*, North Holland, Amsterdam 1985, p. 611.

[11] Z. Stokłosa, P. Kwapuliński, J. Rasek, J. Ilczuk, J. Lelątko, *Acta Phys. Pol. A* **89,** 437 (1996).

[12] G. Herzer, *IEEE Trans. Magn.* **25,** 3327 (1989).

[13] G. Herzer, *IEEE Trans. Magn.* **26,** 1397 (1990).

[14] G. Herzer, *Mater. Sci. Eng. A* **133,** 1 (1991).

[15] G. Herzer, in: *Nanomagnetism*, Ed. A. Hernando, Kluwer Academic Publ., London 1993, p. 111.

[16] G. Herzer, *Scripta Metall. Mater.* **33,** 1741 (1995).